

## Compton scattering of 1.12-MeV gamma rays by $K$ -shell electrons of heavy elements\*

P. P. Kane and P. N. Baba Prasad†

*Department of Physics, Indian Institute of Technology, Powai, Bombay 400 076, India*

(Received 26 November 1975; revised manuscript received 2 June 1976)

A study has been made of the Compton scattering of 1.12-MeV gamma rays by  $K$ -shell electrons of tin, tantalum, gold, lead, and thorium.  $K$  x rays of target atoms were detected in coincidence with the scattered gamma rays. A careful investigation of false coincidences has been carried out. The ratio  $d\sigma_K/d\sigma_F$  of the  $K$ -shell electron cross section to the Compton cross section for a free electron at rest was determined at several angles between  $25^\circ$  and  $120^\circ$ . The cross-section ratio in the case of gold and thorium is less than 1 at  $25^\circ$ , larger than 1 in the neighborhood of  $90^\circ$ , and close to 1 at  $120^\circ$ . The experimental results are compared with theoretical calculations based on the incoherent-scattering-function approximation and a relativistic version of the impulse approximation. There is a need for a comprehensive relativistic calculation incorporating the effects of electron binding in intermediate states.

### I. INTRODUCTION

Compton scattering from  $K$ -shell electrons of atoms of large atomic number  $Z$  is of considerable theoretical and experimental interest. The usual procedure in studies of this process is to use a monoenergetic source of  $\gamma$  rays and to detect a scattered  $\gamma$  ray in coincidence with the  $K$  x ray produced in the target within a short time ( $\sim 10^{-16}$  sec for gold) after the scattering event. Such experiments at an energy as high as 1.12 MeV were described for the first time in a brief report.<sup>1</sup> (References to earlier studies at low energies are given in the same report.)

Important information regarding the process is provided by the differential cross-section ratio  $d\sigma_K/d\sigma_F$ , i.e., the ratio of the differential scattering cross section of a  $K$ -shell electron to that of a free electron initially at rest. The latter cross section is obtained either theoretically from the Klein-Nishina formula or experimentally from Compton scattering measurements in the singles mode with a target of small atomic number. On the assumption that the scattering electrons may be treated as free but moving with velocities characteristic of  $K$ -shell electrons, an impulse approximation (IA) method of analysis was developed particularly for large scattering angles involving large changes of photon momentum. The relativistic formulas of Jauch and Rohrlich<sup>2</sup> for photon scattering from moving electrons were generally used in such analyses.<sup>3-6</sup> However, in our earlier brief report, we have pointed out some of the difficulties associated with this method.

Alternatively, the cross-section ratio has also been compared<sup>4, 7-9</sup> with the incoherent scattering function  $S_K$  for a  $K$ -shell electron. This method is based on the nonrelativistic  $A^2$  approximation in which the  $(e/mc)\vec{p}\cdot\vec{A}$  term in the interaction Ham-

iltonian is neglected and only the  $(e^2/2mc^2)A^2$  term is retained. (Here,  $e, m$ , and  $\vec{p}$  are the charge, mass, and momentum of the electron;  $c$  is the velocity of light, and  $\vec{A}$  is the vector potential of the electromagnetic radiation.) With the help of the closure property,  $S_K$  can be expressed in terms of the form factor  $F_K$  for a  $K$ -shell electron:

$$S_K(q, Z) = 1 - |F_K(q, Z)|^2. \quad (1)$$

Thus, the  $S_K$  method turns out to be appropriate when the form-factor approximation for coherent Rayleigh scattering is appropriate, i.e., for incident photon energies much larger than the electron binding energy but less than  $mc^2$ , and for momentum transfers generally smaller than  $mc$ . Although a detailed justification of the  $S_K$  method has not been given within the framework of a relativistic treatment, Dirac wave functions have been sometimes used<sup>9, 10</sup> to calculate  $S_K$ . The existing tabulations<sup>11</sup> of bound-electron Compton scattering cross sections are based on the nonrelativistic  $S_K$ .

The present study was expected to provide a more stringent test of relativistic aspects than the earlier studies at lower photon energies. In the relativistic theory, the interaction term responsible for photon scattering is  $e\vec{a}\cdot\vec{A}$  and the calculation has to be carried out in the second order of perturbation theory. (Here,  $\vec{a}$  represents the three  $4 \times 4$  Dirac matrices  $\alpha_x, \alpha_y$ , and  $\alpha_z$ .) If one neglects the negative-energy electron states, the  $(e/mc)\vec{p}\cdot\vec{A}$  term is the nonrelativistic analog of the  $e\vec{a}\cdot\vec{A}$  term. Further, the extensive work of Brown and co-workers<sup>12</sup> with respect to Rayleigh scattering from  $K$ -shell electrons has shown that, particularly for large momentum transfer, the relative importance of electron binding in intermediate state increases rapidly with the photon

energy. A similar result should be expected for Compton scattering, although this has not yet been demonstrated unambiguously.

In the theoretical calculations of Henry<sup>13</sup> and Whittingham<sup>14</sup> for 0.662-MeV  $\gamma$  rays, the relativistic formulas of Akhiezer and Berestetskii<sup>15</sup> have been used along with the Furry picture and the Green-function techniques of Brown *et al.* There are a few differences of a technical nature between the two calculations. These are concerned with the methods of performing integrations over angular variables, the numbers of terms retained in Legendre polynomial expansions of the matrix elements and the boundary conditions in the case of absorption first matrix elements for the outgoing electron wave function at large distances. Henry calculates only values of the differential cross section ratio up to an angle of about 60°. The corresponding results of Whittingham cover the entire angular range and are in fairly good agreement with the experiments.

Whittingham's calculation of the energy distribution of Compton scattered photons gives the expected broadening of the Compton peak. The same calculation predicts about 10% shift of the scattered intensity peak position toward higher photon energies with respect to the free Compton line. However, such a shift was not observed by East and Lewis<sup>16</sup> in their experiments with lithium-drifted germanium detectors up to an angle of 70°. In contrast with the exact nonrelativistic calculations of Gavrila<sup>17</sup> for an electron bound in a hydrogen atom, Whittingham does not predict a rise at the low-energy end of the energy distribution down to about 0.1 MeV.

A preliminary study<sup>18</sup> has also been reported of the energy distribution of  $K$ -shell electrons of germanium, released in the Compton scattering of 0.662-MeV  $\gamma$  rays through 135°. With an instrumental width of 0.035 MeV, the width of the measured distribution turned out to be about 0.045 MeV.

The present experiment shows the inadequacy of IA and  $S_K$  approximations, and points to the need for a comprehensive relativistic calculation incorporating the effects of electron binding in intermediate states. Some of the salient details of the experiment are described in Sec. II. The results and conclusions are presented in Sec. III.

## II. EXPERIMENTAL DETAILS

### A. Principle of the experiment

As in the earlier experiments, the events of interest were identified by the detection of the scattered  $\gamma$  rays in coincidence with  $K$  x rays which result within a short time after the scattering.

The differential cross section per unit solid angle,  $d\sigma_K/d\Omega_2$ , for the Compton scattering by a  $K$ -shell electron was measured relative to the differential Compton cross section of a free and stationary electron,  $d\sigma_F/d\Omega_2$ , and the ratio  $d\sigma_K/d\sigma_F$  was determined in each case. Here,  $d\Omega_2$  is a solid angle element in the direction of the scattered photon. The true coincidence rate  $N_t$ , required in the determination of the cross-section ratio, was obtained through Eq. (2):

$$N_t = N - N_c - N_f - N_{eK}, \quad (2)$$

where  $N$  is the coincidence rate measured with the given target,  $N_c$  is the chance coincidence rate,  $N_f$  is the false coincidence rate (measured with an equivalent low- $Z$  target), and  $N_{eK}$  is an estimate of the additional false coincidence rate arising from the simultaneous detection of a  $\gamma$  ray scattered by electrons other than  $K$ -shell electrons and a  $K$  x ray produced by the Compton electron in its passage through the target. Then

$$\frac{d\sigma_K}{d\sigma_F} = \frac{N_t}{N_\gamma} \frac{n_f}{n_K} \frac{\epsilon_\gamma^f}{\epsilon_\gamma^K} \frac{a_\gamma^f}{a_\gamma^K} \frac{1}{\epsilon_K \Omega_K a_K W_K}, \quad (3)$$

where  $N_\gamma$  is the singles counting rate in the  $\gamma$  detector attributable to Compton scattering from an aluminum target,  $n_f$  is the effective number of electrons per unit area of the aluminum target,  $n_K$  is the effective number of  $K$ -shell electrons per unit area of the target under study,  $\epsilon_\gamma^f$  is the detection efficiency of the  $\gamma$  detector for photons Compton scattered by the aluminum target,  $\epsilon_\gamma^K$  is the corresponding detection efficiency for photons Compton scattered by  $K$ -shell electrons of the target under study,  $a_\gamma^f$  is the transmission factor for photons Compton scattered by the aluminum target,  $a_\gamma^K$  is the corresponding factor for photons Compton scattered by  $K$ -shell electrons of the target under study,  $\epsilon_K \Omega_K$  is the efficiency-solid-angle product of the x-ray detector for  $K$  x rays from the target,  $a_K$  is the transmission factor for  $K$  x rays from the target, and  $W_K$  is the  $K$ -shell fluorescence yield of the scattering material. The basis of Eq. (3) has been described by other workers and also by one of the authors.<sup>19</sup> The various quantities on the right-hand side of Eq. (3) were obtained either during the course of the experiment or from published data.

### B. Description of the apparatus

A diagram of the experimental arrangement at 90° scattering angle is given in Fig. 1. A neutron-irradiated cylindrical zinc pellet of 8 mm diameter and 12 mm height served as the zinc-65 source of 1.12-MeV  $\gamma$  rays. It was placed at the center of a cylindrical lead housing of 32 cm di-

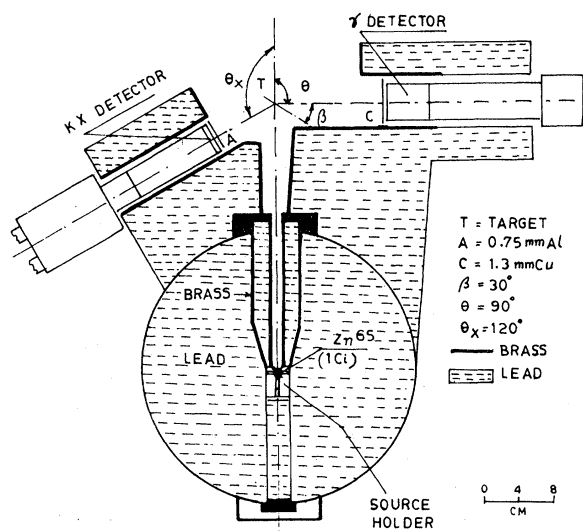


FIG. 1. Experimental arrangement for scattering through  $90^\circ$ .  $\theta$  is the angle of scattering of  $\gamma$  rays.  $\theta_x$  is the angle at which  $K$  x rays of the target are detected.  $\beta$  is the angle between the target plane and the plane normal to the incident beam.

ameter and 32 cm height. The collimator in front of the source had a clear opening of 9.5 mm diameter. Lead surfaces towards the scatterer and the detectors were lined with 12.7-mm or 6.3-mm-thick brass. The strength of the zinc-65 source was approximately 1 Ci after irradiation. Several irradiations were required on account of the long duration of the experiment. It should be noted that the zinc-65 source emits 0.325-MeV positrons with a probability of only 1.5%. The  $K$  x rays were detected by a (38 mm  $\times$  6.3 mm thick) Harshaw NaI(Tl) crystal with a 0.025-mm aluminum cover and mounted on a Dumont 6292 photomultiplier. An additional 0.75-mm-thick aluminum absorber was also used in front of this detector to stop secondary electrons and to attenuate x rays of energy lower than that of  $K$  x rays. The scattered  $\gamma$ -ray detector was a Harshaw integral line assembly consisting of a (44 mm  $\times$  51 mm thick) NaI(Tl) crystal coupled to RCA 6342A photomultiplier. The distance between the center of the source and the target was 32 cm. The x-ray detector was placed at a distance of 8.3 cm from the target and at an angle of  $120^\circ$  with respect to the incident beam. Crystal-to-crystal scattering was considerably minimized by a careful positioning of the shielding blocks. The targets were made from 99.99% pure metals. The circular targets were sandwiched between two thin annular plastic rings whose inner and outer diameters are 4.4 cm and 5.2 cm, respectively. The diameter of the beam spread at the target in a plane perpendi-

cular to the incident beam direction was approximately 2.2 cm. Thus the plastic rings were always well outside the beam. The actual thicknesses of targets, the angles  $\beta$  between the target planes and the plane normal to the incident beam direction, and the distances of the  $\gamma$  detector from the target for different angles of scattering are given in Table I.

The electronic setup was suitable for a conventional coincidence experiment. Energy selection in the case of the x-ray detector was achieved with a single-channel analyzer, the typical window transmission for  $K$  x rays from the target being about 75%. An integral discriminator was used with the scattered  $\gamma$ -ray detector. During the measurements of the cross-section ratio, a resolving time of 0.2  $\mu$ sec was used. During the measurements of the scattered  $\gamma$ -ray pulse height distributions, a fast-slow coincidence system was used in order to produce a gating pulse for a 20-channel pulse height analyzer. The resolving times in the fast and slow branches were 30 nsec and 2  $\mu$ sec, respectively. The performance and the stability of the entire system were checked periodically with the help of 1.17- and 1.33-MeV  $\gamma$  rays from a  $^{60}\text{Co}$  source, and positron-annihilation quanta from a  $^{22}\text{Na}$  source. All the electronic units were run on ac line voltage stabilizers. The ambient temperature was not allowed to vary by more than  $\pm 1^\circ\text{C}$  in relation to the normal value of  $20^\circ\text{C}$ .

### C. Measurements and errors

The experimental procedure has been described in detail by one of the authors.<sup>19</sup> Here only the important points will be mentioned briefly.

The  $\gamma$ -detector bias level was adjusted to pass only pulses with a height well in excess of that corresponding to the mean target  $K$  x-ray energy. This precaution is necessary in order to minimize the counts arising from the detection of  $K$  x rays in the so-called  $\gamma$  detector. The bias levels actually used were 0.300, 0.165, 0.165, 0.110, and 0.100 MeV in the case of measurements at scattering angles of  $25^\circ$ ,  $60^\circ$ ,  $90^\circ$ ,  $100^\circ$ , and  $120^\circ$ , respectively, except that for thorium, at  $100^\circ$  and  $120^\circ$ , the bias levels were 0.145 and 0.165 MeV, respectively. The bias level chosen at an angle corresponds roughly to one-third of the energy of the appropriate "free" Compton line.

The chance coincidence rate was measured by standard techniques. The reasons for false coincidences have been described in detail by Shimizu *et al.*,<sup>4</sup> and East and Lewis.<sup>16</sup> Several types of false coincidences were minimized by the use of relatively thin scattering foils, by the reduction of extraneous material to a min-

imum, and by the placement of shielding blocks around the detectors so that their fields of view were restricted to regions in the vicinity of the target. The secondary electrons were stopped by the use of suitable absorbers in front of the detectors. In the case of the thorium target with the  $\gamma$  detector at  $60^\circ$ , the true coincidence rate per hour dropped from  $142 \pm 10$  for zero absorber to  $34.8 \pm 7.5$ ,  $33.5 \pm 5.4$ , and  $34.9 \pm 3.2$  for 0.275-, 0.825-, and 1.38-mm copper absorbers, respectively, in front of the  $\gamma$  detector. Copper absorbers of 1.38 mm thickness were used for measurements at  $25^\circ$ ,  $60^\circ$ , and  $100^\circ$ . At  $90^\circ$  and  $120^\circ$ , the thickness of the copper absorber was 0.275 mm. As mentioned in Sec. IIB, an aluminum absorber of 0.75 mm thickness was used throughout in front of the x-ray detector.

The false coincidence rate  $N_f$  is usually measured with the substitution of an equivalent aluminum target having the same number of electrons per unit area as the high- $Z$  target under study. The false rate  $N_f$  is then taken as the difference between the coincidence rate measured with such an aluminum target and the corresponding chance coincidence rate. Several target  $Z$ -dependent effects such as bremsstrahlung and coherent  $\gamma$ -ray scattering are not exactly reproduced in this method of estimation of false coincidence

rates. An attempt was made to study this question at  $60^\circ$  in the following way.

Firstly, corresponding to a lead target of  $143.3 \text{ mg/cm}^2$  thickness, the false coincidence rates were measured with equivalent aluminum and copper targets and found to be  $26.30 \pm 0.85$  and  $38.20 \pm 1.07$  per hour, respectively. It should be remembered that, on account of the relatively small copper  $K$ -shell binding energy in relation to the incident  $\gamma$  energy of 1.12 MeV and the relatively narrow pulse height window used with the x-ray detector, there was a negligible probability of true events due to copper  $K$ -shell electrons being registered. Of course the same statement applies, albeit with greater force, in the case of electrons of aluminum. After subtracting the "target out" coincidence rate from these numbers and assuming the differences to be proportional in each case to the square of the target thickness, we calculated the corresponding differences for the thinner targets of aluminum and copper equivalent to a lead target of  $30.3 \text{ mg/cm}^2$  thickness. Then, with the addition of the "target out" coincidence rate, the false coincidence rates for aluminum and copper targets were estimated to be  $18.09 \pm 0.97$  and  $18.54 \pm 0.97$  per hour, respectively, and were found to be in agreement with the rate  $17.83 \pm 0.42$  actually measured

TABLE I. Details regarding the targets and their locations.

Angle of scattering $\theta$ (deg)	Angle of target inclination $\beta$ (deg)	Target	Thickness (mg/cm <sup>2</sup> )	Distance between the target and the $\gamma$ detector (cm)
25	0	Thorium	14.88	21.0
		Gold	12.85	
		Tin	18.80	
60	0	Thorium	14.88	13.0
		Lead	14.01	
		Lead	30.31	
		Lead	143.3	
		Gold	12.85	
		Tin	18.80	
90	30	Thorium	14.88	13.0
		Gold	12.85	
		Tin	18.80	
100	35	Thorium	14.88	13.0
		Lead	143.3	
		Gold	12.85	
120	0	Thorium	14.88	13.0
	0	Gold	12.85	13.0
	40	Gold	19.66	11.0
	40	Gold	34.72	11.0
	0	Tantalum	22.08	11.0

with an equivalent copper target. In view of this agreement, the equivalent aluminum substitution procedure for the determination of false coincidence rates  $N_f$  can be seen to be fairly reliable in the case of targets with thicknesses less than about 30 mg/cm<sup>2</sup>. In any discussion of earlier experiments made with thicker targets, it should be remembered that the same procedure is likely to be unreliable and to underestimate the contribution of the false coincidence rate to the total rate  $N$ .

The rate  $N_{eK}$  can be estimated from a measurement of the Compton singles count rate  $N_{\gamma T}$  with the given target and the known cross section  $\sigma_{eK}$  for  $K$ -shell ionization by electrons. The calculated<sup>20</sup> values of  $\sigma_{eK}$  are known to be in reasonable agreement with the available experimental values<sup>21</sup>:

$$N_{eK} = \frac{Z-2}{Z} N_{\gamma T} N_a \sigma_{eK} \epsilon_K \Omega_K a_K W_K, \quad (4)$$

where  $N_a$  is the number of atoms per unit target area and the other symbols have been defined previously.

Representative data at two angles of scattering for  $N$ ,  $N_c$ ,  $N_f$ ,  $N_{eK}$ , and  $N_t$  are given in Table II. In general, the ratio  $(N_c + N_f)/N$  varied between 0.4 to 0.6 in the case of the 18.80-mg/cm<sup>2</sup> tin target, 0.5 to 0.85 in the case of the 12.85-mg/cm<sup>2</sup> gold target and 0.3 to 0.85 in the case of the 14.88-mg/cm<sup>2</sup> thorium target. The ratio  $N_{eK}/N$  was typically around 0.05 in the case of tin and less than 0.01 in the case of the other targets.

The singles counting rates  $N_\gamma$  were measured with several aluminum targets of thickness up to 202.5 mg/cm<sup>2</sup> and found to be proportional to the thickness. Further, the shapes of the pulse height spectra measured in the singles mode did not show any dependence on the aluminum target thickness. Therefore, multiple scattering is not expected to be significant in the studies described

here.

During the course of the experiment, it was found that the contribution of the natural radioactivity of the thorium target was substantial. Some of the  $\gamma$  rays from thorium, for example of 0.239 and 0.583 MeV, could be clearly recognized from the singles spectrum. The  $\gamma$  rays in association with secondary processes give rise to additional false coincidences during the thorium measurements. These additional false rates were determined in an auxiliary experiment and found to contribute between 30 to 50% of  $N_t$  at each angle.

The contribution of a higher-order process such as the double Compton effect is expected to be less than about 1%. This expectation is confirmed by detailed estimates made on the basis of available experiments<sup>22</sup> and theoretical calculations.<sup>23</sup> Further, the coincidences arising from this effect are taken into account in an approximate way by the "equivalent aluminum subtraction" procedure.

In order to verify whether the experimental value of  $d\sigma_K/d\sigma_F$  was independent of the target thickness, measurements were made with gold targets of different thickness. The results are summarized in Table III. A similar experimental study for targets of different atomic number and at other angles was not considered feasible in view of the long counting periods, the high cost of neutron irradiation, and the 245-day half life of the source. Table III shows that target-thickness-dependent corrections to the differential cross-section ratio are not significant for effective thickness  $\leq 20$  mg/cm<sup>2</sup>.

Pearson's  $\chi^2$  test was used to check the statistical reliability of the data. The error in the cross-section ratio, exclusive of that due to counting statistics, can be estimated through the evaluation of the error in each factor of Eq. (3). The electron number ratio  $n_f/n_K$  was calculated from the

TABLE II. Representative coincidence count rates at two angles (per hour). In some of the cases, additional data were also taken. The significance of  $N$ ,  $N_c$ ,  $N_f$ ,  $N_{eK}$ , and  $N_t$  has been explained in the text immediately after Eq. (2). As outlined in the text, the thorium data for  $N_t$  were finally corrected for the radioactivity contribution. On account of the 245-day half life, the source strengths were quite different for measurements listed in different rows. The effective target thickness is equal to the product of the target thickness and  $\sec\beta$ .

Angle of scattering $\theta$ (deg)	Target and (effective thickness in mg/cm <sup>2</sup> )	Calculated					$N_t = N - N_c - N_f - N_{eK}$
		$N$	$N_c$	$N_f$	$N_{eK}$		
25	Tin (18.80)	20.91 ± 0.60	6.42 ± 0.40	4.38 ± 0.57	1.02	9.09 ± 0.92	
	Gold (12.85)	39.90 ± 0.68	22.36 ± 0.57	11.13 ± 0.78	0.19	6.22 ± 1.09	
	Thorium (14.88)	66.09 ± 1.11	40.31 ± 1.07	16.99 ± 1.41	0.05	8.74 ± 2.09	
90	Tin (21.71)	24.44 ± 0.85	3.00 ± 0.36	7.41 ± 0.62	1.94	12.09 ± 1.11	
	Gold (14.86)	31.30 ± 0.83	7.47 ± 0.50	9.61 ± 0.82	0.27	13.95 ± 1.22	
	Thorium (17.19)	49.76 ± 1.25	15.00 ± 0.91	12.40 ± 1.21	0.40	21.96 ± 1.96	

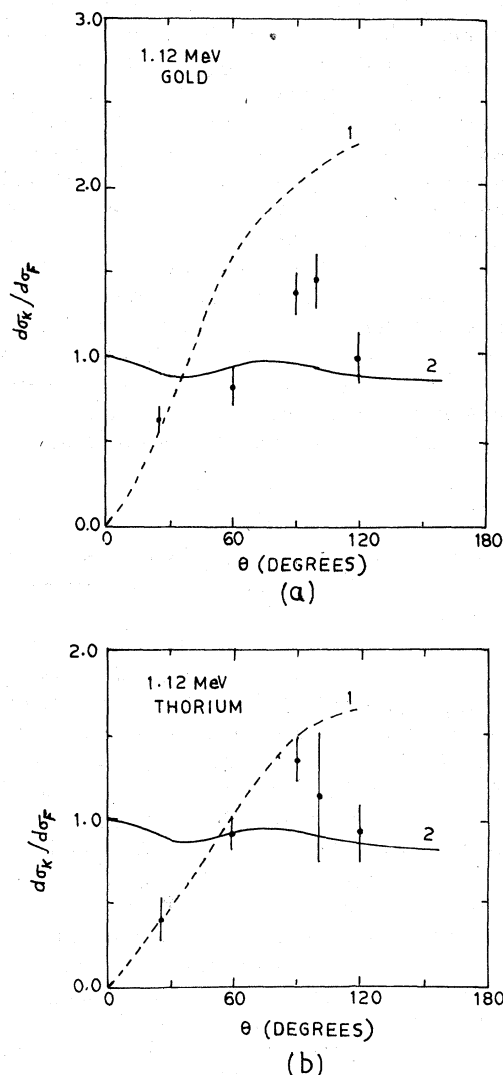
TABLE III. Target-thickness dependence of the differential cross-section ratio for a  $K$ -shell electron.

Angle of scattering $\theta$ (deg)	Target	Effective thickness (mg/cm <sup>2</sup> )	Measured $d\sigma_K/d\sigma_F$
60	Gold	12.85	$0.81 \pm 0.09$
	Lead	14.01	$0.86 \pm 0.10$
	Gold	19.66	$0.90 \pm 0.11$
120	Gold	12.85	$0.98 \pm 0.15$
	Gold	25.65	$1.10 \pm 0.12$
	Gold	45.30	$1.70 \pm 0.18$

measured target thicknesses and should be accurate to better than 2%. The  $\gamma$ -detector efficiency ratio  $\epsilon_V^f/\epsilon_V^K$  and the transmission-factor ratio  $a_V^f/a_V^K$  were estimated to be unity within 5% and 1%, respectively. The values<sup>24</sup> of the  $K$ -shell fluorescence yield  $W_K$  are believed to be accurate to about 1%. The error in the product  $\epsilon_K \Omega_K a_K$  has been estimated to be about 10% and is the main component of the systematic errors. The combined error in the cross-section ratio, exclusive of that due to counting statistics, hardly affects the relative values at different angles and is about 12%.

TABLE IV. Comparison of the experimental values of the differential cross-section ratio for a  $K$ -shell electron with approximate theoretical values at 1.12 MeV. Values of  $d\sigma_K/d\sigma_F$  in the fourth column were calculated according to a relativistic version of the IA method as outlined in Ref. 1. Values of  $S_K$  in the fifth column were calculated according to the formula of Shimizu *et al.* in Ref. 4.

Target (thickness in mg/cm <sup>2</sup> )	$\theta$ (deg)	$d\sigma_K/d\sigma_F$		$S_K$
		Experiment	IA method	
Tin (18.80)	25	$0.71 \pm 0.07$	0.97	1.49
	60	$0.86 \pm 0.08$	0.98	4.41
	90	$0.94 \pm 0.08$	0.99	5.77
Tantalum (22.08)	120	$0.91 \pm 0.26$	0.91	2.74
Gold (12.85)	25	$0.63 \pm 0.09$	0.93	0.56
	60	$0.81 \pm 0.09$	0.94	1.58
	90	$1.33 \pm 0.12$	0.95	2.05
	100	$1.44 \pm 0.15$	0.94	2.09
	120	$0.98 \pm 0.15$	0.90	2.28
Lead (14.01)	60	$0.86 \pm 0.10$	...	1.45
Thorium (14.88)	25	$0.40 \pm 0.13$	0.90	0.42
	60	$0.91 \pm 0.11$	0.92	1.15
	90	$1.36 \pm 0.12$	0.93	1.49
	100	$1.20 \pm 0.39$	0.91	1.56
	120	$0.93 \pm 0.15$	0.87	1.66

FIG. 2. Angular variation of the differential cross-section ratio at 1.12 MeV for (a) gold and (b) thorium. The curves labeled 1 are calculated on the basis of the non relativistic  $S_K$  formula of Shimizu *et al.* (Ref. 4). The curves labeled 2 are calculated on the basis of a relativistic version of the impulse approximation (Ref. 1). The experimental data are shown by solid circles along with statistical errors.

### III. RESULTS AND CONCLUSIONS

The measured values of the differential cross-section ratio are given in Table IV which differs in several respects from a similar one presented in our earlier brief report.<sup>1</sup> The values obtained at 60° in the case of lead and at 100° are new. All the values have now been corrected for the contribution of the rate  $N_{eK}$  to the total coincidence rate  $N$ . Further, some of the values have been revised slightly. Results presented in the fourth

and fifth columns of Table IV represent values of the ratio calculated respectively by the relativistic IA method and by the  $S_K$  method according to the formula of Shimizu *et al.* It should be noted that several  $S_K$  values are larger than unity and much larger than the corresponding experimental values. The disagreement is perhaps not surprising in view of the limited range of applicability of the incoherent scattering function approximation. Further, the calculated values in the fourth column are less than unity and are also in poor agreement with the data. The situation can be seen at a glance in Figs. 2(a) and 2(b) drawn for gold and thorium, respectively. For scattering angles  $\approx 120^\circ$  involving large momentum transfers, the differential cross-section ratio  $d\sigma_K/d\sigma_F$  approaches unity. The calculations of Whittingham for 0.662-MeV  $\gamma$  rays indicate a similar trend. However, it should be mentioned that the accuracy of the numerical computations such as those of Whittingham becomes progressively poorer with increasing momentum transfer.

We believe we have shown, at an energy of the order of  $\approx 1$  MeV, the need for a comprehensive relativistic calculation incorporating the effects of electron binding in intermediate states. If the calculation is made along the lines suggested by Whittingham, a larger number of terms in the Legendre polynomial expansion will have to be

calculated in view of the higher  $\gamma$  energy. The radial integrals in such calculations contain discrete and continuum state solutions of the Dirac equation. Whether the point Coulomb potential is an adequate representation of the potential experienced by the scattering electron is an important question in these calculations. For the momentum transfers with which we are usually concerned in the Compton scattering of 1.12-MeV  $\gamma$  rays, the immediate neighborhood of a nucleus is expected to make the dominant contribution to the integrals. The electron wave functions in this region<sup>25</sup> differ from the pure Coulombic form only in a normalization factor. The resultant screening correction to the cross sections is expected to be less than 2%. Whether any correlation effects should also be considered in the theoretical evaluation is an open question that cannot be settled at the present time.

#### ACKNOWLEDGMENTS

We wish to thank M. S. Biderkundi for the preparation of gold foils, workshop personnel under the supervision of K. Shridhara for fabrication of apparatus, and K. S. Kulkarni and R. M. Nayak for assistance in computer programming. We acknowledge helpful discussions with Professor R. H. Pratt of the Department of Physics, University of Pittsburgh, Pittsburgh, Pa.

\*Work supported in part by a grant from the National Bureau of Standards, Washington, D.C. under the PL-480 program.

†Part of this work was submitted by P. N. Baba Prasad in partial fulfilment of the requirements for the Ph.D. degree of the Indian Institute of Technology, Bombay.

<sup>1</sup>P. N. Baba Prasad and P. P. Kane, *J. Res. Nat. Bur. Stand., Sec. A* **78**, 461 (1974).

<sup>2</sup>J. M. Jauch and F. Rohrlich, *The Theory of Photons and Electrons* (Addison-Wesley, Reading, Mass., 1955), p. 222-230.

<sup>3</sup>J. W. Motz and G. Missoni, *Phys. Rev.* **124**, 1458 (1961).

<sup>4</sup>S. Shimizu, Y. Nakayama, and T. Mukoyama, *Phys. Rev.* **140**, A806 (1965).

<sup>5</sup>A. Ramalinga Reddy, K. Parthasaradhi, V. Lakshminarayana, and S. Jnanananda, *Ind. J. Pure Appl. Phys.* **6**, 255 (1968).

<sup>6</sup>D. V. Krishna Reddy, E. Narasimhacharyulu, and D. S. R. Murthy, *Physica* **75**, 394 (1974).

<sup>7</sup>O. Pingot, *Nucl. Phys. A* **119**, 667 (1968).

<sup>8</sup>O. Pingot, *Nucl. Phys. A* **133**, 334 (1969).

<sup>9</sup>Z. Sujkowski and B. Nagel, *Arkiv Fys.* **20**, 323 (1961).

<sup>10</sup>B. Talukdar, S. Mukhopadhyaya, and D. Chattarji, *Phys. Lett.* **35A**, 37 (1971).

<sup>11</sup>J. H. Hubbell, Wm. J. Veigele, E. A. Briggs, R. T. Brown, D. T. Cromer, and R. J. Howerton, *J. Phys. and Chem. Ref. Data* **4**, 471 (1975), and earlier tabu-

lations mentioned therein. For example Wm. J. Veigele, *At. Data* **5**, 51 (1973).

<sup>12</sup>G. E. Brown and J. B. Woodward, *Proc. Phys. Soc. (Lond.) A* **65**, 977 (1952); G. E. Brown, R. E. Peierls, and J. B. Woodward, *Proc. Roy. Soc. (Lond.) A* **227**, 51 (1954); and G. E. Brown and D. F. Mayers, *Proc. Roy. Soc. (Lond.) A* **242**, 89 (1957).

<sup>13</sup>E. M. Henry, Ph.D. thesis (University of Colorado, 1969) (unpublished).

<sup>14</sup>I. B. Whittingham, *J. Phys.* **4**, 21 (1971).

<sup>15</sup>A. I. Akhiezer and V. B. Berestetskii, *Quantum Electrodynamics* (Interscience, New York, 1955).

<sup>16</sup>L. V. East and E. R. Lewis, *Physica* **44**, 595 (1969).

<sup>17</sup>M. Gavril, *Phys. Rev. A* **6**, 1348 (1972); **6**, 1360 (1972).

<sup>18</sup>M. Pradoux, H. Meunien, J. Bauman, and G. Roche, *Nucl. Inst. Meth.* **112**, 443 (1973).

<sup>19</sup>P. N. Baba Prasad, Ph.D. thesis (Indian Institute of Technology, Bombay, 1975) (unpublished).

<sup>20</sup>B. L. Moiseiwitsch and S. J. Smith, *Rev. Mod. Phys.* **40**, 238 (1968).

<sup>21</sup>D. H. Rester and W. E. Dance, *Phys. Rev.* **152**, 1 (1966); and H. Kolbenstvedt, *J. Appl. Phys.* **38**, 4785 (1967).

<sup>22</sup>M. R. McGie and F. P. Brady, *Phys. Rev.* **167**, 1186 (1968), and earlier references mentioned therein.

<sup>23</sup>F. Mandl and T.H.R. Skryme, *Proc. Roy. Soc. (Lond.) A* **215**, 497 (1952).

<sup>24</sup>A. H. Wapstra, G. J. Nijgh, and R. Van Lieshout, *Nuclear Spectroscopy Tables* (North-Holland, Amsterdam, 1959); and W. Bambynek, B. Crasemann, R. W. Fink, H. U. Freund, H. Mark, C. D. Swift, R. E.

Price, and P. Venugopala Rao, *Rev. Mod. Phys.* 44, 716 (1972).

<sup>25</sup>R. H. Pratt, A. Ron, and H. K. Tseng, *Rev. Mod. Phys.* 45, 273 (1973).